NURETH14-360

BENCHMARKS FOR INTERFACE-TRACKING CODES IN THE CONSORTIUM FOR ADVANCED SIMULATION OF LWRs (CASL)

D. Chatzikyriakou¹, J. Buongiorno¹ and D. Lakehal^{1,2}

¹ Massachusetts Institute of Technology, USA

² ASCOMP GmbH, Switzerland

despoina@mit.edu, jacopo@mit.edu, lakehal@ascomp.ch

Abstract

A major innovation pursued by the Consortium for Advanced Simulation of LWRs (CASL) is the use of Interface Tracking Methods (ITM) to generate high-fidelity closure relations for two-phase flow and heat transfer phenomena (e.g. nucleate boiling, bubble break-up and coalescence, vapor condensation, etc.), to be used in coarser CFD, subchannel and system codes. ITMs do not assume an idealized geometry of the interface between the liquid and vapor phases, but rather calculate it from 'first principles'. Also, used within the context of high-fidelity turbulence simulations, such as Direct Numerical Simulation (DNS) or Large Eddy Simulation (LES), ITMs can resolve the velocity (including the fluctuating field) and temperature/scalar gradients near the liquid-vapor interface, so prediction of the exchange of momentum, mass and heat at the interface in principle requires no empirical correlations. The physical complexity of the two-phase flow and heat transfer phenomena encountered in LWRs naturally lends itself to an ITM analysis approach.

Several codes featuring ITM capabilities are available within CASL. These are TransAT, STAR-CCM+, PHASTA, FTC3D and FELBM. They use a variety of ITMs ranging from Volume-Of-Fluid to Level-Set, from Front-Tracking to Lattice-Boltzmann. A series of benchmark simulations is being developed to test the key capabilities of these codes and their ITMs. In this paper, three such benchmark simulations, testing DNS, LES and interface tracking, respectively, are briefly described.

Keywords: two-phase flow and heat transfer, LES, DNS, interface tracking

1. Introduction

Thermal-hydraulic research activities within the Consortium for Advanced Simulation of LWRs (CASL) project focus on the development of high-fidelity simulation capabilities for subcooled boiling heat transfer in PWR fuel assemblies. The traditional modeling approaches for subcooled boiling are highly empirical, relying in particular on empirical heat transfer coefficient correlations to calculate the vapor generation term at the wall, and then simple semi-empirical models for bubble drag, condensation, breakup and coalescence are used, all assuming idealized geometries of the vapor/liquid interface, i.e. spherical or elliptical or otherwise symmetric bubbles [1]. The physical reality of the situation is of course much more complex, as shown by direct visualization of the phenomena (see **Figure 1**). The topology of the liquid/vapor interface is highly irregular and its nature is dynamic; also, rapid changes in interface topology generate turbulence, which cannot be captured by the traditional statistical turbulence models.

CASL is developing multiphase CFD capabilities in the form of the Eulerian phase-averaged multi-fluid flow framework without interface tracking. Examples of such approach are the Eulerian Multi-Phase (EMP) module in the STAR-CD code, the mixture algebraic slip module in the TransAT and NPHASE codes. These models require closure relations for the phase-to-phase and wall-to-flow mass, momentum and energy interaction terms in the governing equations. In the mixture algebraic slip model, a further closure for the drift flux is needed. A major innovation pursued by CASL is the use of Interface Tracking Methods (ITM) to generate high-fidelity closure relations for the multiphase CFD code. The relative domains of the CFD and ITM approaches are depicted in **Figure 1** for subcooled flow boiling.

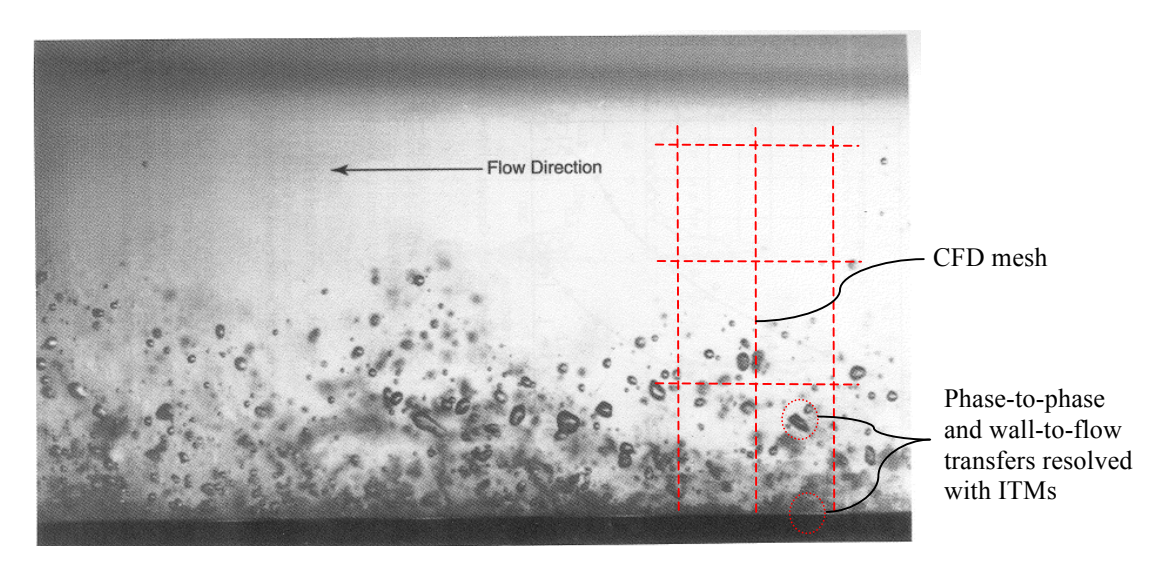


Figure 1. Bubble layer in high-subcooling, high-mass-flux, high-pressure, flow boiling of Freon near the point of DNB. The situation is qualitatively similar to the PWR hot fuel assembly (from Tong and Tang [2]).

ITMs do not assume an idealized vapor-liquid interface topology, but rather calculate it from 'first principles'. A marker function C is introduced, its value being zero if vapor is present at position \vec{r} at time t, and one if liquid is present:

$$C(\vec{r},t) = \begin{cases} 1 & liquid \\ 0 & vapor \end{cases}$$
 (1)

The marker function, which effectively defines the interface between the two phases, is predicted by a topology equation [3]:

$$\frac{\partial C}{\partial t} + \vec{u} \cdot \nabla C = \frac{\dot{m}}{\rho} \delta_{S} \tag{2}$$

where \vec{u} is the velocity vector of the interface, \vec{m} is the phase-change rate, ρ is the density and δ_s is the Dirac delta function at the interface. Different ITMs differ in how the topology equation is solved; the state-of-the-art approaches are Volume Of Fluid (VOF) [4-6], Level Set (LS) [7, 8] Front Tracking (FT) [9, 10] and the Lattice-Boltzmann Method [11-13]. ITMs are coupled with

an appropriate 'flow solver' for the velocity, pressure and temperature fields. In the presence of turbulence, various approaches are possible such as Direct Numerical Simulation (DNS), Large Eddy Simulation (LES), or Unsteady Reynolds Averaged Navier Stokes (URANS). The reader is referred to the enormous amount of information about these methods which can be found in the CFD literature. Since the velocity and temperature gradients near the interface can be resolved, prediction of the exchange of momentum, mass and heat at the interface in principle requires no empirical correlations. Examples of ITM simulations performed with the code TransAT are shown in **Figure 2**. It can be seen that in all cases the interface can be resolved quite sharply.

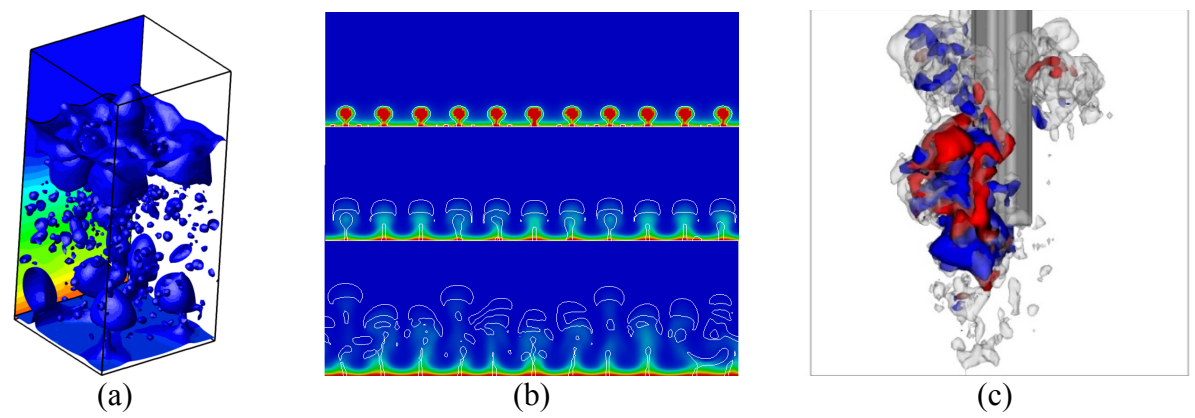


Figure 2. (a) Level-Set simulation of film boiling from a flat surface in a reduced domain (courtesy of Ascomp), (b) Level Set simulation of film boiling from a flat surface in a wider domain, showing more heterogeneous topology modes at various instants (courtesy of Ascomp), and (c) LES-VOF simulation of gas injection in a BWR suppression pool of water [14].

In CASL, five codes with ITM capabilities are currently being evaluated; namely:

- 1) Finite Element Lattice Boltzmann Method (FELBM) code by City College of New York
- 2) Front Tracking Code 3D (FTC3D) by Notre Dame University
- 3) Parallel Hierarchic Adaptive Stabilized Transient Analysis (PHASTA) code by Rensselaer Polytechnic Institute
- 4) STAR-CCM+ by CD-Adapco
- 5) TransAT by Ascomp GmbH

The key characteristics of the codes are summarized in **Table 1**.

2. Testing the capabilities of the ITM codes

A series of benchmark simulations has been defined to test the key capabilities of the ITM codes available to CASL. The benchmarks are meant to (i) focus on phenomena relevant to the actual PWR hot assembly physical situation, (ii) test key interface-tracking and turbulence simulation capabilities required to probe these phenomena, and (iii) build an adequate database (experimental or 'numerical') for model validation. **Table 2** reports the set of benchmarks currently under detailed definition. In this paper we focus on the description of Benchmarks #1, 2 and 3b, which have been developed by the authors.

The 14th International Topical Meeting on Nuclear Reactor Thermal Hydraulics (NURETH-14) Hilton Toronto Hotel, Toronto, Ontario, Canada, September 25-29, 2011.

Code Name	-,	FELBM	FTC3D	PHASTA	STAR-CCM+	TransAT
Code Developer		CCNY	Notre Dame Univ.	RPI	CD-adapco	Ascomp GmbH
ITM Used		LBM	FT	LS	VOF	LS, VOF, phase field
	Phase-to-phase	Yes	Yes	No	Yes	Yes
Heat Transfer	Wall-to-flow	Yes	Yes	Yes	Yes	Yes
	Within solid	Yes	Yes	No	Yes	Yes
Mass Transfer (evaporation,	Phase-to-phase	Yes	Yes	No	Yes	Yes
condensation)	Wall-to-flow	Yes	Yes	No	Yes (correlation)	No
Subgrid Models		No	Microlayer, thin films, mass transfer boundary layer	No	No	Microlayer, interfacial thermal resistance, interfacial turbulence
Turbulence Models (beyond DNS)		LES	None (DNS)	LES, RANS	LES, V-LES, URANS, RANS	LES, V-LES, URANS, RANS
Time Discretization (accuracy)		Explicit (2 nd order)	Predictor-corrector, pressure projection (2 nd order)	Implicit (2 nd order)	Implicit (up to 2 nd order)	RANS implicit (2 nd order), LES and ITM explicit (up to 5 th order)
Space Discretization (accuracy)		Finite elements (up to 4 th order)	Centered differences and ENO (2 nd order)	Finite elements (2 nd order)	Upwind (2 nd order), HRIC (for VOF)	ENO-WENO for ITM (up to 5 th order)
Mesh Topologies		Body-fitted unstructured, hex and tetra	Structured Cartesian grids	Unstructured and adaptive meshes	Any cell shape and mesh topology	Cartesian, body-fitted, immersed surface technology (IST) with block-mesh refinement
Demonstrated Scalability		75% efficiency for 1000 finite elements per node	No recent results available	81% efficiency when going from ~4100 to ~164000 processors	Up to 2000 nodes with 10 ⁹ cells	~100% efficiency up to 160 nodes, more scalability tests underway
Code Source		Open	Open	Open	Proprietary	Proprietary
GUI Preprocessing (grid)		Not built-in (can use Gambit)	None (grid specified in input file)	Simapps libraries for mesh generation and (C) Simmetrix GUI to set up problem BCs and ICs.	Extensive CAD to volume mesh capabilities included	Built-in pre-processor for IST and Cartesian meshes
GUI Postprocessing (view)		Not built-in (can use Tecplot)	Not built-in (can use Tecplot, Paramesh)	Not built-in (can use Solidworks, Paraview)	Built-in post-processor	Not built-in (can use Tecplot, Paraview, OpenDX)

Table 1. General characteristics of the CASL ITM codes

Physical	Benchmark	Objective	Relevance	Capabilities tested
phenomena	case #	•		Capabilities testeu
Single-phase turbulence and heat	1	Predict friction factor of turbulent flow over a flat wall with a pattern of small hemispherical solid obstacles	Subcooled boiling in PWR hot channel at axial locations between the onset of nucleate boiling and the point of net vapor generation	Single-phase CFD without interface tracking, heat and phase change
transfer	2	Predict axial location of onset of subcooled nucleate boiling (point where $T_w \approx T_{sat}$) in bundle unit cell with uniform heat flux	Onset of nucleate boiling in PWR hot channel	Single-phase CFD with heat transfer, but without interface tracking and phase change
	3a	Predict growth and detachment of single air bubble under flow conditions	Subcooled boiling in PWR hot channel before and after point of net vapor generation	Interface-tracking and CFD, no heat transfer and phase change
Single bubble	3b	Predict growth and detachment of single bubble under saturated pool boiling conditions	Subcooled boiling in PWR hot channel before and after point of net vapor generation	Interface-tracking and CFD with heat transfer and phase change (evaporation only) including a microlayer evaporation model
	3c	Predict growth and detachment of single bubble under subcooled flow boiling conditions	Subcooled boiling in PWR hot channel before and after point of net vapor generation	Interface-tracking and CFD with heat transfer and phase change (both evaporation and condensation) including a microlayer evaporation model
Multiple bubbles 4		Predict the void fraction distribution dependency on bubble deformability in a turbulent up-flow	Subcooled boiling in PWR hot channel after net vapor generation	Interface tracking and CFD, no heat transfer and no phase change

Table 2. Summary of ITM benchmarks in CASL

2.1 Benchmark # 1

In the PWR hot channel, beyond the onset of nucleate boiling but before the point of net vapor generation, small vapor bubbles are attached to the fuel rods [15]. Heat and mass are transferred by evaporation from the base to the tip of the bubbles where condensation occurs; therefore, the heat transfer coefficient increases with respect to single-phase flow conditions. Also, the bubbles, effectively, act as surface roughness and thus, depending on their size, may affect the friction coefficient and ultimately the flow distribution across the subchannels within the fuel assembly. In this benchmark, the focus is on the effect of the attached bubbles on near-wall

turbulence and friction coefficient. Heat transfer and phase change are not part of this benchmark.

The simulation domain is shown in Figure 3. It consists of a Cartesian box with small hemispherical obstacles attached to the upper and lower walls, effectively representing the bubbles attached to the PWR fuel rods. Several simplifications with respect to the PWR situation were introduced to facilitate performance of the benchmark case simulations. First, since the bubble diameter is small compared to the channel width, the effect of rod curvature can be neglected, thus a configuration of turbulent flow over a flat wall is deemed an acceptable representation of the curved surface situation. Second, since the shear Reynolds number (222-2*22h2, u* is the friction velocity (m/s), 22h is the half channel height (m) and 2 is the kinematic viscosity of the fluid (m²/s)) for the PWR channel is Re_r~10⁴, performing a DNS or LES simulation for such high Re, is computationally prohibitive. As such, the benchmark problem was scaled down to more reasonable flow conditions, namely Re_r = 400 for which both DNS and LES simulations are manageable with current computational resources [16]. This choice of Re, also enables comparison of the results to existing DNS databases for single-phase flow over smooth and rough surfaces at the exact same flow conditions [17, 18]. Third, the bubbles are actually treated as solid hemispherical obstacles, thus no interface tracking is needed for this benchmark. The main difference is that for a solid obstacle the no-slip boundary condition applies, while for an actual bubble it does not, as the flow perceives the interface differently from a wall. However, it was suggested in the literature that slip effects for this problem are insignificant [19].

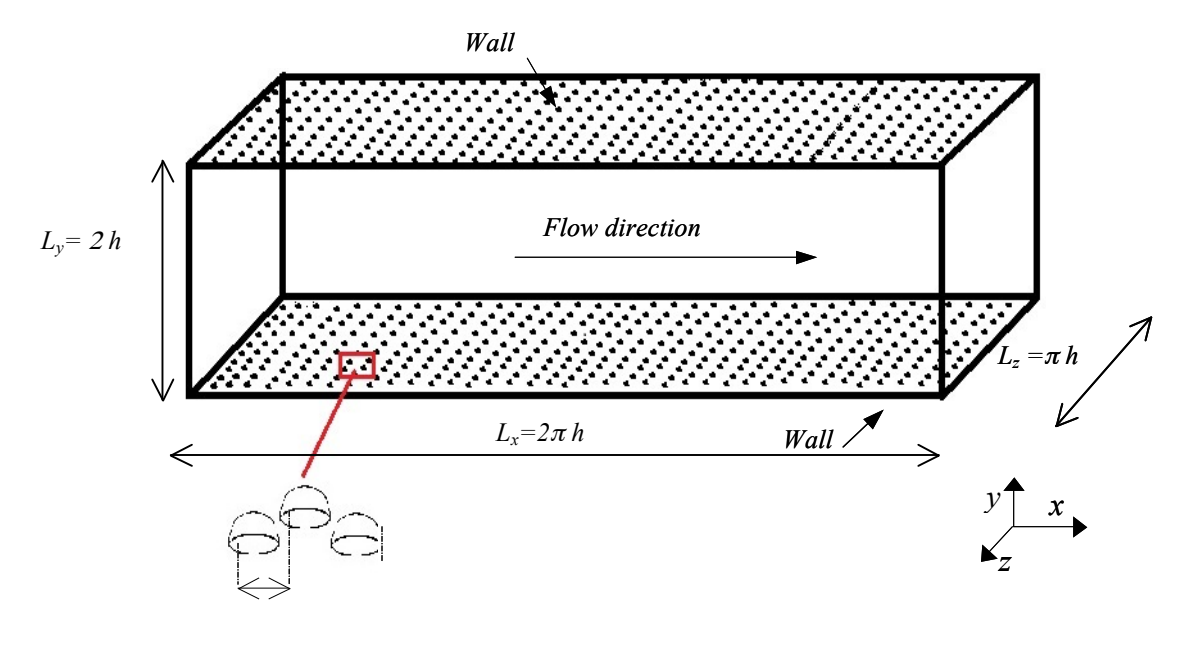


Figure 3. Computational domain for benchmark case 1

The fully-developed turbulent channel flow is homogeneous in the streamwise and spanwise directions. Periodic boundary conditions can thus be used for the fluid flow in the streamwise and spanwise directions, x and z, respectively. The computational domain (period) was chosen to include the largest eddies in the flow [20] and such that the turbulent eddies are not correlated. Wall conditions (no-slip) are applied at the lower and upper horizontal planes of the channel. In

DNS and LES, a pressure gradient dp/dx should be imposed in the x-momentum equation (as a source term), to generate the flow, adjusted to obtain $Re_i = 400$.

Using a fluid with properties representative of water at PWR conditions (ρ = 710 kg/m³ and μ = 9×10⁻⁵ Pa·s), the participants in this benchmark are expected to perform at least two calculations, i.e. channel flow with no obstacle (reference case), and channel flow with obstacles, and to report the following quantities from those simulations: (i) mean and r.m.s velocity profiles, (ii) mean shear stress profiles, (iii) turbulent stresses anisotropy, (iv) turbulent kinetic energy (TKE) and dissipation near the wall, (v) Reynolds stress and TKE budgets, (vi) friction coefficient. The results from the reference case simulation can be compared to the database (experimental and numerical) from Ashrafian et al. [17] and Krogstad et al. [18]. However, no experimental data exist for flow over hemispherical obstacles at the conditions of interest outlined above. An *ad-hoc* numerical database will be generated by MIT using DNS (code TransAT). A grid independence study should be performed both for the DNS and the LES computations. The size and the type of the grid around the hemispherical obstacles will depend on the specific code used.

Initial LES simulations (code TransAT) of flow in a channel with no obstacles, for *Re*=400, show very good agreement with DNS data available in the literature [18]. Both the mean velocity and shear stress profiles obtained with the LES simulation are very close to the DNS predictions (**Figure 4**). Two subgrid scale models were used for the LES simulation: the Smagorinsky model under low-Re flow conditions (including a near-wall damping), and the WALE variant of Nicoud and Ducros [21].

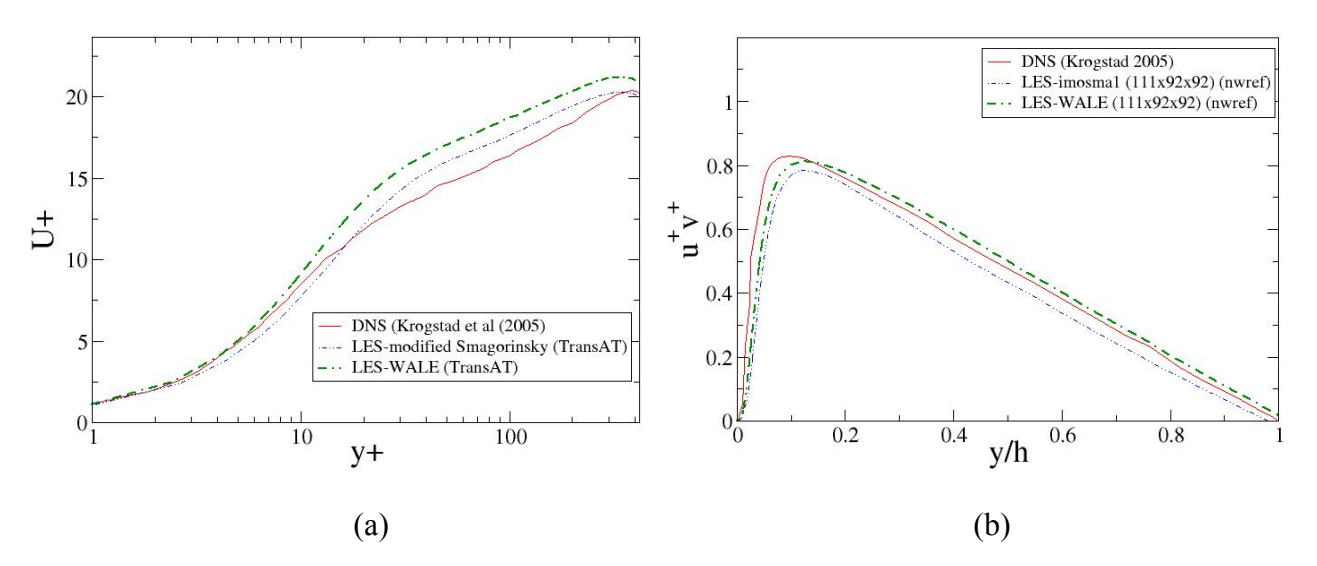


Figure 4. LES-DNS comparison for flow in channel without obstacles (Re=400). (a) Dimensionless mean axial velocity and (b) Dimensionless < u'v' > Reynolds stress

2.2 Benchmark #2

The onset of nucleate boiling in PWR hot channels occurs when the temperature of the heated rod slightly exceeds saturation. The surface temperature of the heated rods gradually increases along the flow direction until the temperature of nucleation is reached. In this benchmark case, the focus is on the single-phase convective heat transfer phenomena leading up to the onset of nucleate boiling. Interface tracking and phase change are not part of this benchmark.

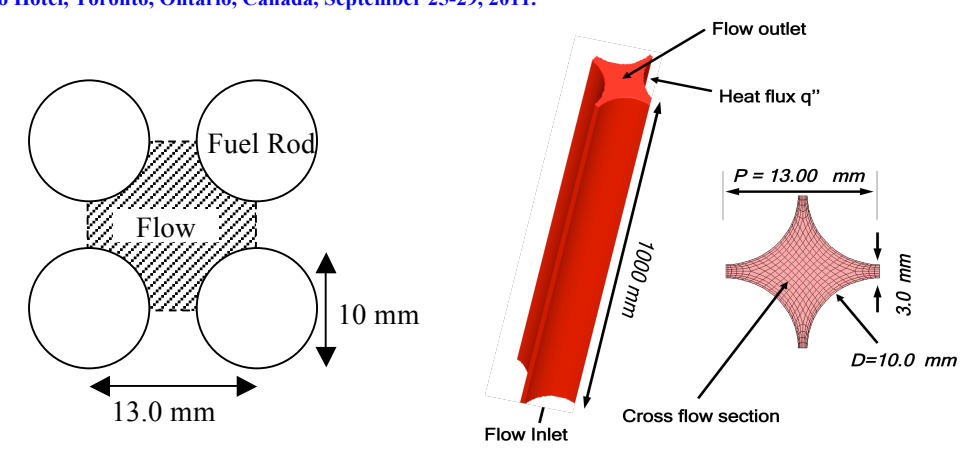


Figure 5. Computational domain for benchmark 2

Benchmark 2 is inspired by the PBST OECD (OECD/NRC Benchmark based on NUPEC PWR Sub-channel and Bundle Tests (PSBT)) single subchannel benchmark [22]. Several simplifying assumptions were introduced to facilitate performance of the simulations. First, the temperature of nucleation was assumed to be equal to the saturation temperature. Second, a reasonably low shear Reynolds number, Re=300, was selected to make both DNS and LES simulations affordable. Third, the length of the domain was shortened to 1 m, to relax the meshing requirements in the axial direction. Since the distance to the onset of nucleate boiling depends on the integrated power (heat flux times rod surface area) supplied to the fluid, the heat flux was also scaled accordingly.

For a fluid with properties representative of PWR water (ρ = 710 kg/m³, μ = 9×10⁻⁵ Pa·s, k= 0.54 W/m-K, c_p = 5.9 kJ/kg-K), the participants in this benchmark are expected to run a simulation for the thermal-hydraulic conditions reported in **Table 3**. The following quantities should be extracted and reported: the length at which the surface temperature of the rod reaches the saturation temperature, i.e. distance to the onset of nucleate boiling (X_{ONB}), length of thermal and momentum entry regions, PSD (Power Spectral Density) energy spectra at X_{ONB} , heat transfer coefficient at X_{ONB} .

Pressure	15.5 MPa		
Saturation temperature	344.6 °C		
Inlet temperature	290 °C		
Mass flux	74.1 kg/m ² s (corresponding to Re=300)		
Heat Flux	50 W/m^2		

Table 3. Operating flow conditions for benchmark 2.

Periodic boundary conditions in the spanwise directions should be applied to mimic the effect of the neighboring rods. Wall conditions (no-slip) should be applied at the rod surface. In the axial direction, this is a space evolving flow and as such it requires an inflow-outflow set-up. There exist various ways to impose inflow conditions, one of which is based on digital filtering [23], which is recommended.

The heat transfer coefficient results can be compared to the predictions of the well established heat transfer coefficient correlations for fully-developed turbulent flow of water in a rod bundle, e.g., the Dittus-Boelter correlation with the Weisman correction factor to account for the effect of bundle geometry [24].

The results sample presented in **Figure 6** were obtained with the code TransAT using the V-LES approach to simulate the unsteady turbulent flow with convective heat transfer along one rod, under radial cyclic conditions. The rod is heated with a constant volumetric heat source. The Reynolds number is quite high in this case (Re~10⁶), which justifies the use of V-LES. The same exercise will be conducted within Benchmark 2, using LES instead of V-LES, but for a lower Reynolds number.

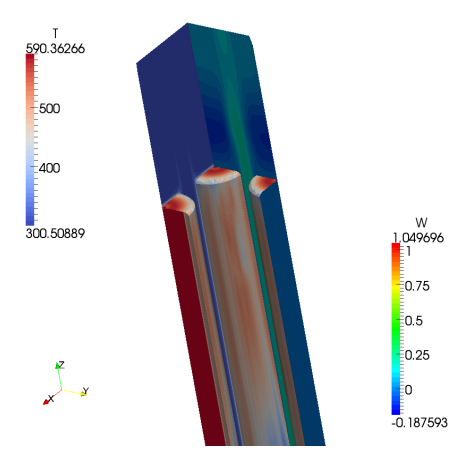


Figure 6. V-LES simulation of the flow and (conjugate) heat transfer along the heated rod (TransAT simulations)

2.3 Benchmark #3b

As a first step towards modeling bubble growth and detachment in subcooled flow boiling in the PWR hot assembly, Benchmark 3b focuses on the simplified case of a single steam bubble growing at a heated wall, under saturated pool-boiling conditions at atmospheric pressure. Thus, interface tracking, heat transfer and phase change are part of this benchmark, but the effects of condensation and imposed flow are not.

The ebullition cycle can be qualitatively described as follows. Conduction heat transfer elevates the temperature of the liquid adjacent to the wall. Once the liquid reaches the superheat required to activate a nucleation site, a bubble begins to form and pushes the surrounding liquid outward, except for a thin liquid microlayer (whose thickness is of the order of 5-10 µm) that remains in contact with the wall underneath the bubble. In this first phase of the ebullition cycle, bubble growth is driven by the pressure imbalance across the vapor/liquid interface, and is resisted by the liquid inertia. Once the interfacial pressure imbalance subsides, bubble growth is driven mainly by the intense evaporation occurring at the bubble surface and through the microlayer. When the size of the bubble is sufficiently large, buoyancy causes the bubble to detach from the wall; fresh liquid floods the wall, and the cycle starts over. Upon bubble detachment, considerable agitation takes place within the liquid near the wall, a phenomenon referred to as microconvection, which enhances the overall heat transfer. A depiction of the important heat transfer mechanisms during bubble growth is shown in **Figure 7**.

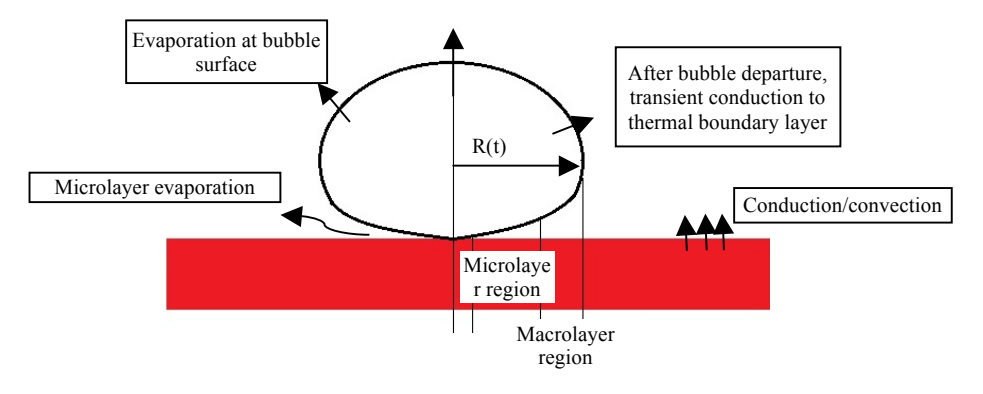


Figure 7. Schematic of vapor bubble growing at the heated wall

The computational domain for benchmark 3b simulations is shown in **Figure 8**. It includes the fluid (both liquid and vapor phases) and the solid wall. The conjugate heat transfer problem has to be solved throughout the whole domain. An isolated bubble is essentially an axisymmetric system, where the vertical axis of the bubble is the axis of symmetry. At the conditions of interest, steam bubbles typically have a departure radius of the order of \sim 1 mm. The size of the domain was chosen to eliminate end effects. The boundary conditions at r=2 mm and at the top of the domain (z=3 mm) are set to open or pressure boundary conditions, where the pressure is fixed at atmospheric conditions (i.e. reference value). The boundary condition at the wall (z=0.4 mm) is no slip. All the domain boundaries can be considered adiabatic.

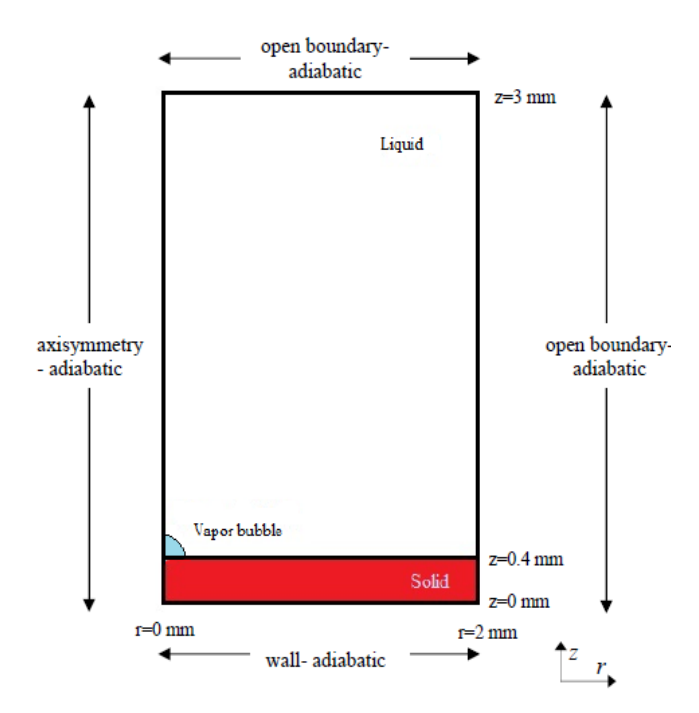


Figure 8. The computational domain for benchmark 3b. (Drawing not to scale)

Figure 9 shows the results from a preliminary simulation performed with the code TransAT, using the level-set method for the bubble-liquid interface tracking and the immersed surface technique for the representation of the solid substrate.

The geometry, materials and simulation parameters were chosen to enable validation against an *ad-hoc* database to be generated at the MIT pool boiling facility, shown in **Figure 10** and extensively described in a separate paper to be presented at NURETH-14. This facility uses a combination of high-speed infrared thermometry, digital video and Particle Image Velocimetry (PIV) to measure the temperature, phase and velocity distributions in the proximity of a boiling surface.

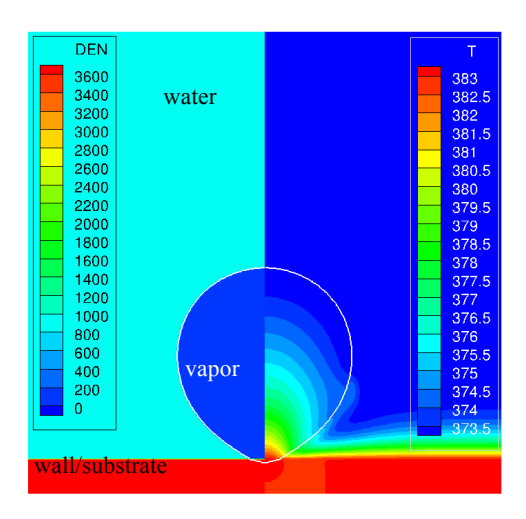


Figure 9. Preliminary 2D axisymmetric bubble-growth simulation using level-set in TransAT, showing different materials (substrate-liquid-vapor) with density contours (in kg/m^3) (left) and temperature distribution (in degrees K) (right). The bubble is about to depart from the substrate with a diameter of ~1.8 mm.

The following assumptions and initial conditions can be adopted in the simulation of this system:

- Because the ITO (Indium-Tin-Oxide) heater is so thin compared to the sapphire substrate, its thermal capacity and resistance can be neglected when modeling the conjugate heat transfer within the wall. Heat generation within the ITO should be modeled as a constant planar heat generation rate, $q=50 \text{ kW/m}^2$, imposed at z=0.4 mm.
- The Reynolds number is low, so laminar flow is expected.
- The initial velocity can be assumed to be zero throughout the domain.
- The initial pressure in the liquid should be atmospheric plus the hydrostatic term.
- Simulation of the actual micro-cavity from which the bubble would nucleate is beyond the scope of this benchmark. Therefore, to start the bubble growth simulation, a small bubble has to be 'seeded' at a prescribed location on the wall, with a prescribed nucleation temperature of $T_n=110$ °C.
- A static contact angle in the range 80-90° should be specified at the solid-liquid-vapor triple contact line, as measured (at room temperature) on the actual heaters in the facility.
- A uniform temperature should be prescribed within the sapphire substrate, equal to T_n , and a temperature equal to the saturation temperature (T_{sat} =100°C) in the liquid far from the wall (z>1.4 mm), with an appropriate interpolation within the fluid near the wall (1 mm<z<1.4 mm). The participants in this benchmark should try several different initial temperature distributions and verify that after cyclic conditions are achieved (within ~2-3 ebullition cycles), the solution is independent of the initial temperature distribution selected.

To allow for a meaningful evaluation of the results, the participants should extract and report the following quantities (all as functions of time): bubble shape (i.e. interface marker iso-contours), bubble volume (or equivalent radius), velocity field in the liquid around the bubble, temperature field on the wall surface, bubble rising velocity after detachment. Experimental data will be available for validation of these quantities, as generated in the facility shown in **Figure 10**.

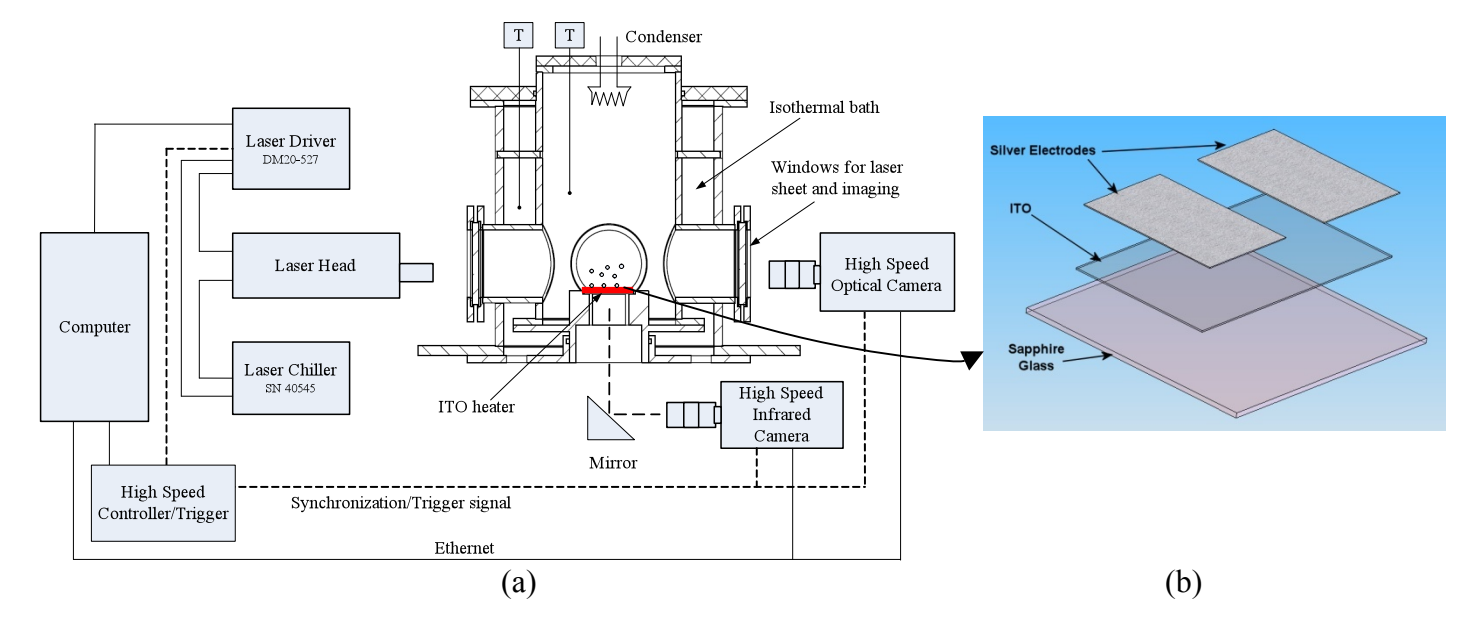


Figure 10. (a) The MIT pool boiling facility. Lateral and bottom access ports are provided for the PIV laser beam, high-speed video camera and infrared camera, respectively. When a dichroic mirror is used, a second digital video camera can be placed under the heater to image the boiling process from below. (b) Exploded view of the heater piece. The Indium-Tin-Oxide (ITO) heater is deposited on top of the sapphire substrate. Two silver electrodes deliver the electric current to the ITO, which area exposed to the boiling fluid is $30 \times 10 \text{ mm}^2$.

3. Conclusions

CASL seeks to advance the state-of-the-art of LWR thermal-hydraulics simulation through the systematic use of ITMs. In this paper, three benchmarks to test the flow, heat transfer, interface tracking and phase change capabilities of the ITM codes used in CASL were briefly described. These benchmarks are:

- Fully-developed turbulent flow over a flat surface with hemispherical obstacles,
- Developing turbulent flow within a (short) PWR-like subchannel, and
- Single bubble growth and detachment from a hot wall in a stagnant pool of saturated liquid

A detailed description of these benchmarks can be found in the CASL reports, available upon request from co-author J.B. At the time of this paper preparation, the benchmark simulations are underway. The results will be reported in future publications.

4. Acknowledgements

This work is supported by the U.S. Department Of Energy (DOE) through the Consortium for Advanced Simulation of Light Water Reactors (CASL) project. CD-adapco (Dr. E. Baglietto),

City College of New York (Profs T. Lee and M. Kawaji), University of Notre Dame (Prof. G. Tryggvason) and Rensselaer Polytechnic Institute (Prof. M. Podowski) are gratefully acknowledged for providing the information about their codes.

5. References

- [1] M. Ishii and T. Hibiki, "Thermo-fluid dynamics of two-phase flow", Springer, 2006
- [2] L. S. Tong and Y. S. Tang, "Boiling heat transfer and two-phase flow", 328-336, 1997
- [3] D. Lakehal, M. Meier and M. Fulgosi, "Interface tracking towards the direct simulation of heat and mass transfer in multiphase flows", *Int. J. Heat and Fluid Flow*, Vol. 23, No. 2002, pp. 242-257.
- [4] R. Scardovelli and S. Zaleski, "Direct numerical simulation of free-surface and interfacial flow", *Ann. Rev. Fluid Mech.*, Vol. 31, No. 1999, pp. 567—603.
- [5] M. Rudman, "A volume-tracking method for incompressible multifluid flows with large density variations", *Int. J. Numer. Meth. Fluids* Vol. 28, No. 1998, pp. 357–378.
- [6] W. J. Rider and D. B. Kothe, "Reconstructing volume tracking", *J. Comp. Phys.*, Vol. 141, No. 1998, pp. 112-152.
- [7] S. J. Osher and R. P. Fedkiw, "Level set methods: An overview and some recent results", *J. Comp. Phys.*, Vol. 169, No. 2001, pp. 463-502.
- [8] J. A. Sethian, "Evolution, implementation and application of level set and fast marching methods for advancing fronts", *J. Comp. Phys.*, Vol. 169, No. 2001, pp. 503-555.
- [9] J. Du, B. Fix, J. Glimm, X. Jia, X. Li, Y. Li and L. Wu, "A simple package for front tracking", *J. Comp. Phys.*, Vol. 213, No. 2006, pp. 613-628.
- [10] G. Tryggvason, B. Bunner, A. Esmaeeli, D. Juric, N. Al-Rawahi, W. Tauber, J. Han, S. Nas and Y.-J. Jan, "A front tracking method for the computations of multiphase flow", *J. Comp. Phys.*, Vol. 169, No. 2001, pp. 708—759.
- [11] N. Takada, M. Misawa, A. Tomiyama and S. Fujiwara, "Numerical simulation of two- and three-dimensional two-phase fluid motion by lattice boltzmann method", *Computer Physics Communications*, Vol. 129, No. 1-3, 2000, pp. 233-246.
- [12] K. Sankaranarayanan, X. Shan, I. G. Kevrekidis and S. Sundaresan, "Bubble flow simulations with the lattice boltzmann method", *Chemical Engineering Science*, Vol. 54, No. 21, 1999, pp. 4817-4823.
- [13] T. Inamuro, T. Ogata, S. Tajima and N. Konishi, "A lattice boltzmann method for incompressible two-phase flows with large density differences", *Journal of Computational Physics*, Vol. 198, No. 2, 2004, pp. 628-644.
- [14] P. Liovic and D. Lakehal, "Interface-turbulence interactions in large-scale bubbling processes", *Int. J. Heat and Fluid Flow*, Vol. 28, No. 2007, pp. 127-144.
- [15] J. G. Collier and J. R. Thome, "Convective boiling and condensation", O. S. Publications, 3rd Edition, 1996
- [16] Z. Xie and I. Castro, "Les and rans for turbulent flow over arrays of wall-mounted obstacles", *Flow, Turbulence and Combustion*, Vol. 76, No. 3, 2006, pp. 291-312.
- [17] A. Ashrafian, H. I. Andersson and M. Manhart, "Dns of turbulent flow in a rod-roughened channel", *International Journal of Heat and Fluid Flow*, Vol. 25, No. 3, 2004, pp. 373-383.
- [18] P.-Å. Krogstad, H. I. Andersson, O. M. Bakken and A. Ashrafian, "An experimental and numerical study of channel flow with rough walls." *J. Fluid Mech*, Vol. 530, No. 2005, pp. 327-352
- [19] D. B. R. Kenning and M. G. Cooper, "Interfacial circulation due to surface-active agents in steady two-phase flows", *J. Fluid Mech.*, Vol. 24, No. 2, 1966, pp. 293-306.

- [20] J. Kim, P. Moin and R. Moser, "Turbulence statistics in fully developed channel flow at low reynolds number", *J. Fluid Mech.*, Vol. 177, No. 1987, pp. 133-166.
- [21] F. Nicoud and F. Ducros, "Subgrid-scale stress modelling based on the square of the velocity gradient tensor", *Flow, Turbulence and Combustion*, Vol. 62, No. 1999, pp. 183-200.
- [22] A. Rubin, A. Schoedel and M. Avramova, "Oecd/nrc benchmark based on nupec pwr subchannel and bundle tests;vol. I: Experimental database and final problem specifications", NEA/NSC/DOC(2010)1 (November 2010)
- [23] M. Klein, A. Sadiki and J. Janicka, "A digital filter based generation of inflow data for spatially developing direct numerical or large eddy simulations", *J. Comp. Phys.*, Vol. 186, No. 2003, pp. 652-665.
- [24] J. Weisman, "Heat transfer to water flowing in parallel tube bundles", *Nuclear Science and Engineering*, Vol. 6, No. 1, 1959, pp. 78-79.